Marine Geology 449 (2022) 106819

Contents lists available at ScienceDirect

Marine Geology

journal homepage: www.elsevier.com/locate/margo

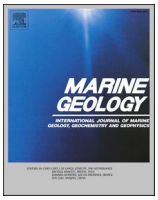

Potential fields modeling for the Cayos Basin (Western Caribbean Plate): Implications in basin crustal structure

Ana Maria Osorio-Granada [a,b,c], Bismarck Jigena-Antelo [a,*], Juan Manuel Vidal Pérez [a], Orlando Hernández-Pardo [b], Hermann León-Rincón [c], Juan J. Muñoz-Pérez [a]

[a] Universidad de Cádiz, Campus de Puerto Real, CASEM, Puerto Real, Cadiz, Spain
[b] Universidad Nacional de Colombia, Department of Geosciences, Bogotá D.C., Colombia
[c] Oceanographic and Hydrographic Research Center of Colombia, Cartagena, Colombia

ARTICLE INFO

Keywords:
The Cayos Basin
The Caribbean Sea
Gravity and magnetic anomalies
Marine geophysics

ABSTRACT

The Cayos Basin is an offshore basin located in the Colombian Caribbean Sea and forms part of the Lower Nicaraguan Rise, a geological province of the western region of the Caribbean Plate. Until now, the origin of the province is still being debated. Advanced research in the study area regarding its composition and structure, from land outcrops, petrology and geochemistry of drilled cores and dredged samples, and geophysical investigations, indicates a volcanic origin for this geological province, and a close relationship to the formation of the Caribbean Large Igneous Province. On the contrary, other studies suggest that the Lower Nicaraguan Rise may be part of the continental Chortis block. In this paper, we present and discuss alternative scenarios for the nature of the underlying crust below the sedimentary sequences in the Cayos Basin. We characterize the basin through the interpretation of magnetic and gravity anomaly grids, and 2D forward modeling, constructed based on three sections, by considering restriction seismic data from previous works. The results show that the Cayos Basin is underlain by geological bodies with high density and higher magnetization. From the gravity and magnetic forward modeling, we estimated the depth to the basement is about 2–6 km, and the Moho discontinuity to have an average of 18 km below, the Cayos Basin. Our investigation implies that, at least, the Cayos Basin is in the oceanic crust domain and shows no evidence of a continental source of the Chortis block.

1. Introduction

The Cayos basin is a marine frontier basin located in the western region of the Colombian Caribbean Sea. The geometry of the basin has been established by the National Hydrocarbon Agency (Barrero et al., 2007) and represents a total area of 144,755 km^2. The Cayos Basin is bounded to the south and southeast by the Colombia Basin. To the west, it is limited by the Upper Nicaraguan Rise and continental lands of Central America, and to the northeast, the basin extends to the Jamaican Caribbean islands (Fig. 1).

The basin includes water depths of up to 4000 meters, nine oceanic islands (San Andres, Providencia, and Santa Catalina), atolls and coral banks (Cayos de Roncador Island, Cayos de Quitasueño Island, Cayos de Serrana Island, Cayos del Este Sudeste Island, Cayos de Albuquerque Island, Cayos de Serranilla Island, among others) that reach variable elevations above sea level, with a maximum altitude of circa 360 m at the Providencia Island (León-Rincón et al., 2019; Rey et al., 2021). The seafloor exhibits a rough and variable morphology with diverse types of submarine landforms, such as ridges, troughs, and seamounts. The elevation model of the Cayos Basin reaches depths of between approximately −2908 and − 4407 m, showing a deepening to the east (Fig. 2).

Geological studies have concluded that the atolls, islands, and coral banks within the Cayos Basin may have originated in Early Cenozoic times as volcanoes (Christofferson and Hamil, 1978; Wadge and Wooden, 1982; Case et al., 1990; Holcombe et al., 1990a; Mauffret and Leroy, 1997; Carvajal Arenas and Mann, 2018; Restrepo-Alvarez et al., 2014). The subsidence of these volcanoes and simultaneous capping by shallow-water carbonate deposits, from the Cenozoic through the Quaternary, gave rise to the formation of the shallow banks and atolls (Geister, 1992). Geophysical studies suggest that most coral banks, atolls, and islands, within the basin, are part of the province known as Lower Nicaraguan Rise (LNR). The LNR is considered as a crustal block, between the Upper Nicaraguan Rise (UNR) to the northwest, and the Colombia Basin to the southeast (Holcombe et al., 1990b; Mauffret and

* Corresponding author.
E-mail address: bismarck.jigena@gm.uca.es (B. Jigena-Antelo).

https://doi.org/10.1016/j.margeo.2022.106819
Received 25 October 2020; Received in revised form 31 March 2022; Accepted 8 May 2022
Available online 13 May 2022

Leroy, 1997) (Fig. 2). Research on the structure and tectonic development of this province has been formulated since the 1990s, and is still being debated (Case et al., 1990; Restrepo-Alvarez et al., 2014). It is an ongoing discussion whether the LNR may be part of the continental Chortis Block (Dengo, 1985; Krawinkel and Seyfried, 1994; Hradecky, 2011) or, in contrast, may be composed of oceanic crust, as suggested by several authors (Case et al., 1990; Holcombe et al., 1990a; Mauffret and Leroy, 1997; Muñoz et al., 1997). Most Caribbean researchers refer to the LNR as a portion of the Caribbean Large Igneous Province (CLIP) that has largely been controlled by the accumulation of sediments, structural deformation of the existing crust, and volcanism (Case et al., 1990; Mauffret and Leroy, 1997; Mauffret and Leroy, 1999; D'Acremont et al., 2003; Rogers et al., 2007; Boschman et al., 2014; Carvajal Arenas and Mann, 2018; Sanchez et al., 2019).

The aim of this paper is to report the results obtained by the integration of gravimetric and magnetic data (Berrocoso et al., 1996; Jigena et al., 2016), incorporating seismic profiles of the Cayos basin in the LNR. Anomaly maps and 2D gravity/magnetic forward modeling have been used to reveal the general crustal structure and to discriminate between oceanic and continental crust blocks and near-surface sedimentary elements. Moreover, the current hypothesis assuming that the studied area is part of the continental Chortis block, will be checked.

2. Tectonic and geological setting

The present-day configuration of the western Caribbean has been recognized as an important constraint on the tectonic origin and evolution, registering the history of displacement from the Cretaceous to the Cenozoic. Most authors now agree that the Caribbean Plate was formed during the Late Cretaceous in the eastern Pacific region, with migration eastwards, relative to the North and South American plates behind an east-facing Great Arc of the Caribbean, to its present position.

The geological history of the Cayos Basin in the LNR is not known in detail. Previous studies (Geister, 1992; Muñoz et al., 1997; Idarraga Garcia and Leon Rincon, 2019) have reported that it appears to be an oceanic crustal block, bounded by the Pedro Bank Fault Zone in the northwest, and, the Hess Escarpment Fault Zone in the southeast. Faults, seismic activity, small-displacement deformation, and recent volcanism in the seafloor of the area suggest a continuous and active microplate boundary in the LNR along the San Andres Rift and Hess Escarpment Fault Zone (Carvajal Arenas and Mann, 2018). The intraplate deformation within de Caribbean plate shows structural features within the upper crust and sedimentary sections typical of other active rifts.

Seismic reflection data appear to indicate that most of the deposits that cover the LNR, including the Cayos Basin, are pelagic, with a section ranging in thickness from 500 to 1000 m (Bowland and Rosencrantz, 1988; Holcombe et al., 1990b; Mann and Burke, 1990). The basement configuration displays volcanic structures in the form of horst and grabens that control the sedimentation in local basins (Carvajal and Mann, 2015).

The structural features in the study area have been taken from the previously geophysical studies (Carvajal Arenas, 2017; Sanchez et al., 2019) and include the Nicaraguan Rise, the Hess Escarpment Fault Zone, the Pedro Bank Fault Zone, the San Andres Rift, the Colombian Basin, and several islands, banks, atolls, and seamounts (Fig. 1). These features will be discussed in the next sections.

2.1. The Nicaraguan Rise

The Nicaraguan Rise is located across the Caribbean Sea, from the coast of Honduras and Nicaragua to Jamaica. It is a NE-SW trending modern carbonate platform with deep-water basins and is divided into the Upper (or Northern) and Lower (or Southern), by the left lateral Pedro Bank Fault Zone (Fig. 2) (Case et al., 1990; Ott et al., 2013). The Upper Nicaraguan Rise is a structural high, extending from Central America eastward to Jamaica, and consists of the Chortis Block (Arden Jr, 1969). The Lower Nicaraguan Rise, with a probable volcanic origin (Case et al., 1990), appears to be an oceanic crustal block, part of the Caribbean Large Igneous Province (CLIP) (Mauffret and Leroy, 1997).

2.2. The Hess Escarpment Fault Zone

The Hess Escarpment Fault Zone is defined as a late Cretaceous left-lateral, strike-slip fault, active during the period when the Caribbean

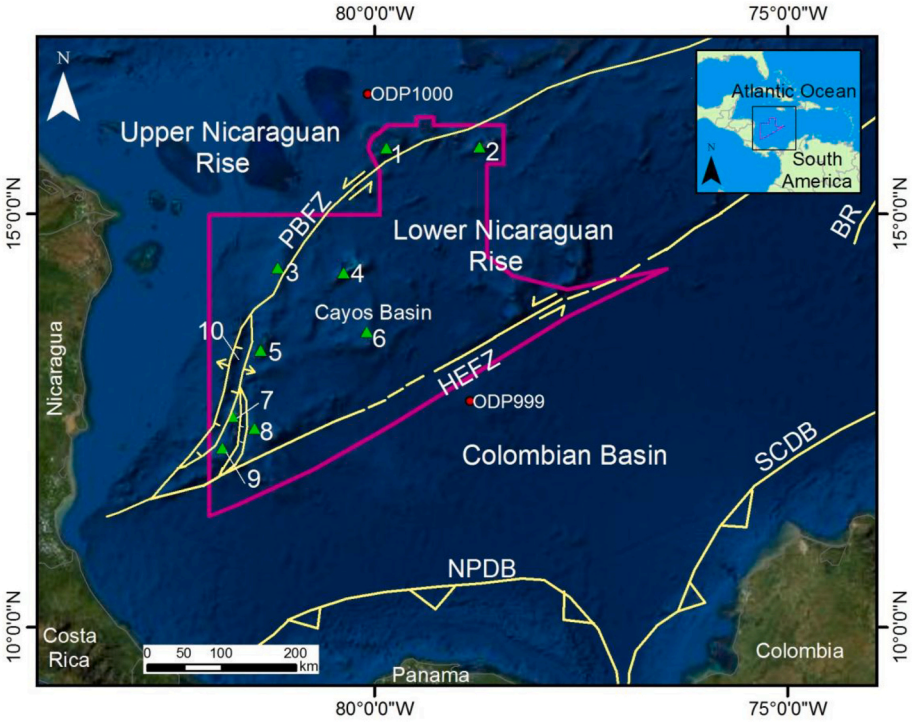

Fig. 1. Localization of the Cayos Basin in a regional map of the Western Caribbean Sea showing tectonomorphologic features of the study area, which include fault zones and lineaments, areas of active rifting or seafloor spreading, and convergent plate zones (From Carvajal Arenas, 2017). The study area is shown delineated in pink (Barrero et al., 2007). The green triangles show atolls, islands, and coral banks. The red circles show drilled wells. Seismic lines are displayed in red. Abbreviations: BR: Beata Ridge. NPDB: North Panama Deformed Belt. PBFZ: Pedro Bank Fault Zone. SCDB: South Caribbean Deformed Belt. 1. Cayos de Serranilla Island. 2. Cayos de Bajo Nuevo Island. 3. Cayos de Quitasueño Island. 4. Cayos de Serrana Island. 5. Providencia Island. 6. Cayos de Roncador Island. 7. San Andrés Island. 8. Cayos de Este Sudeste Island. 9. Cayos de Albuquerque Island. 10. San Andres Rift. (For interpretation of the references to colour in this figure legend, the reader is referred to the web version of this article.)

plate was being transported from the eastern Pacific into the present day position (Burke, 1988; Holcombe et al., 1990a). Idarraga Garcia and Leon Rincon (2019) describe major fault systems along the its trace: Albuquerque-Turmeque Fault, Mono Fault, and Hess Fault where the Hess Escarpment represent the main and single geomorphological expression on the seafloor (Fig. 2).

2.3. The Pedro Bank Fault Zone

The Pedro Bank Fault Zone corresponds to another lineament within the study area (Fig. 2), with an important N30°E and N62°E trending and a left-lateral component (Case et al., 1990; Holcombe et al., 1990a; Carvajal Arenas, 2017). Idarraga Garcia and Leon Rincon (2019) define four major fault systems: Albuquerque-Providencia, Pedro, Quitasueño, and Serrana.

2.4. The San Andres Rift

The San Andres Rift corresponds to a bathymetric and structural rift basin, with a structural trend of N15°E, within the Caribbean Plate (Carvajal Arenas, 2017) (Fig. 2). The pull-apart basin opened from Eocene to recent as a result of left-lateral motion on the Pedro Banks fault to the northeast (Holcombe et al., 1990b).

2.5. The Colombian Basin

The Colombian Basin is limited to the south by the South Caribbean Deformed Belt, to the northwest by the LNR, to the west by the North Panama Deformed Belt, and by the Beata Ridge to the east. The Colombian Basin is underlain by the CLIP (Burke, 1988) with an approximate crustal thickness of between 10 and 18 km (Ewing et al., 1960).

2.6. Islands, banks, and atolls of the Archipelago

According to Geister (1992), most coral banks, atolls, and islands of the Archipelago of San Andrés, Providencia, and Santa Catalina (San Andrés, and Providence Islands, Cayos de Roncador Island, Cayos de Quitasueño Island, Cayos de Serrana Island, Cayos del Este Sudeste Island, Cayos de Albuquerque Island, Cayos de Serranilla Island, among others within the Cayos Basin) may have originated through volcanic activity during the Early Cenozoic (Geister and Díaz, 2002). Subsidence and simultaneous capping of these volcanoes by shallow-water carbonate layers, from the Cenozoic through the Quaternary, gave rise to the formation of the shallow banks and atolls of the basin (Geister and Díaz, 2002).

3. Dataset and methods

The crustal analyses of the Cayos Basin in the LNR were largely inferred from morphological or bathymetric changes in the seafloor, and the gravity and magnetic datasets. All grids were processed by using Geosoft Oasis Montaj software utilities, and minimum curvature interpolation was applied to generate maps and profiles.

3.1. Bathymetric data

Bathymetric data were obtained from the ETOPO datasets. The data integrates land topography and ocean bathymetry from the National Oceanic and Atmospheric Administration (NOAA) (Amante and Eakins, 2009). The analysis of the digital elevation model (DEM) was sampled between the longitudes 83.3 W° to 75.6 W° and latitudes 10.7 N° to 16.7 N°.

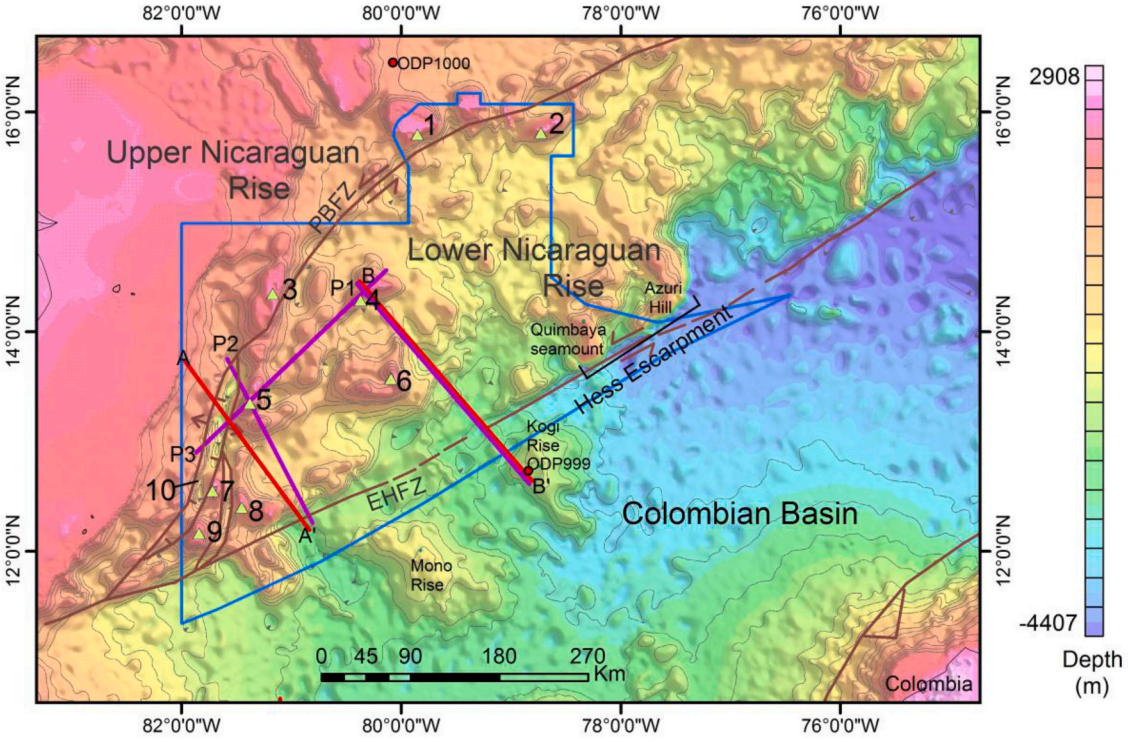

Fig. 2. Digital elevation model (DEM) of the Cayos Basin showing major tectonic features. The locations of 2D gravity and magnetic profiles are displayed as purple lines. The red line indicates the location of the seismic profiles. The red circles show drilled wells. 1. Cayos de Serranilla Island. 2. Cayos de Bajo Nuevo Island. 3. Cayos de Quitasueño Island. 4. Cayos de Serrana Island. 5. Providencia Island. 6. Cayos de Roncador Island. 7. San Andrés Island. 8. Cayos de Este Sudeste Island. 9. Cayos de Albuquerque Island. 10. San Andres Rift. Bathymetric data from ETOPO1 grid dataset (Amante and Eakins, 2009) (For more references see Fig. 1). (For interpretation of the references to colour in this figure legend, the reader is referred to the web version of this article.)

3.2. Gravity data

We use gravity data acquired by a shipborne geophysical survey, conducted in the Colombian Caribbean Sea, by Fugro Geoteam AS. The survey is known as the Cayos Basin area (Caribbean). The area consisted of 2939 km of gravity data, acquired on-board the M/V Polar Venturer. The survey production period was from October 15, 2005, to November 11, 2005. The onboard gravity data was corrected for latitude, the drifting of the equipment, the Eötvös effect and a reduction density of 2670 kg/m^3 and sea level were used as a datum. The products resulting from the work, described herein, compile information on the digital terrain model, Bouguer gravity, and free-air gravity anomaly.

As already known, the Bouguer gravity anomaly needs to be decomposed into its regional and residual component sources, before making any interpretation (Heiskanen and Moritz, 1967; Hofmann-Wellenhof and Moritz, 2005). In this research, we applied the trend surface method to approximate the regional component of the gravity field (Menke, 2012). The trend was removed by applying an orthogonal polynomial surface of third-order to the Bouguer grid. We obtained a residual Bouguer anomaly map, linked to medium and long wavelengths, that could be related to the middle and lower crustal densities.

3.3. Magnetic data

The magnetic data was obtained from the Decade of North American Geology (DNAG), published by (Bankey et al., 2002), between the longitudes 83.3 W° to 75.6 W° and latitudes 10.7 N° to 16.7 N°. We used offshore data acquired from the National Geophysical Data Center of the National Oceanic and Atmospheric Administration and which span the years 1958 through 1997. According to Bankey et al. (2002), and Oviedo Prada et al. (2021), only total magnetic field data were used, to which diurnal corrections, when available, had already been applied. The DGRF was then removed, using the date of the original surveys. Merging surveys was achieved by computational draping, using sea level as a datum and applying the method of Cordell (1992). In our work, we used the total anomaly of the magnetic field for analysis. This grid was performed to a final cell size of 1 km using a minimum curvature algorithm. We minimized the polarity effects from the magnetic anomaly by applying the Reduction-to-the-pole filtering technique (Blakely and Simpson, 1986) using an average latitude of 14°N. The operation centers the magnetic anomalies over their causative features, making the interpretation easier and more reliable.

3.4. Seismic and well data

For this study we combined interpretations from 2D-reflection seismic profiles (see Fig. 2 for location), made by Carvajal Arenas and Mann (2018) and Sanchez et al. (2019), to correlate the physical properties with a geological model for the Cayos Basin region.

The interpretation of the seismic profile A-A' with a SW-NE trending (Fig. 3) (Carvajal Arenas and Mann, 2018) was based on: 1) the correlation of wells available in the Nicaraguan Rise (Abrams and Hu, 2000; Carvajal and Mann, 2015; Carvajal Arenas, 2017); and, 2) interpretation of available 2-D auxiliary seismic data and other works from previous authors (Holcombe et al., 1990b; Bowland, 1993; Carvajal Arenas et al., 2013). Carvajal Arenas and Mann (2018) converted the time domain in depth by using the method of Layer Cake Depth Conversion (Marsden, 1989).

The Fig. 4 displays an uninterpreted and interpreted seismic profile B-B′ across the Cayos Basin (Sanchez et al., 2019), with ages based on the description of the well ODP-999. Well ODP-999 (see Fig. 2 for location) is tied to the seismic profile in the Colombian Basin. Correlations with the reflection seismic record were constrained by comparison to synthetic seismograms, calculated using downhole sonic velocity (DSV), and density data and the far-field source wavelet represented by the seafloor reflection (Abrams and Hu, 2000).

3.5. 2D forward gravity modeling

The forward modeling along the Cayos Basin area was calculated using the GM-SYS module of Oasis Montaj. GM-SYS creates synthetic models through the computation of anomalies caused by an n-sided polygon in two dimensions (Talwani and Heirtzler, 1964). Several polygons constitute each model and represent different geological

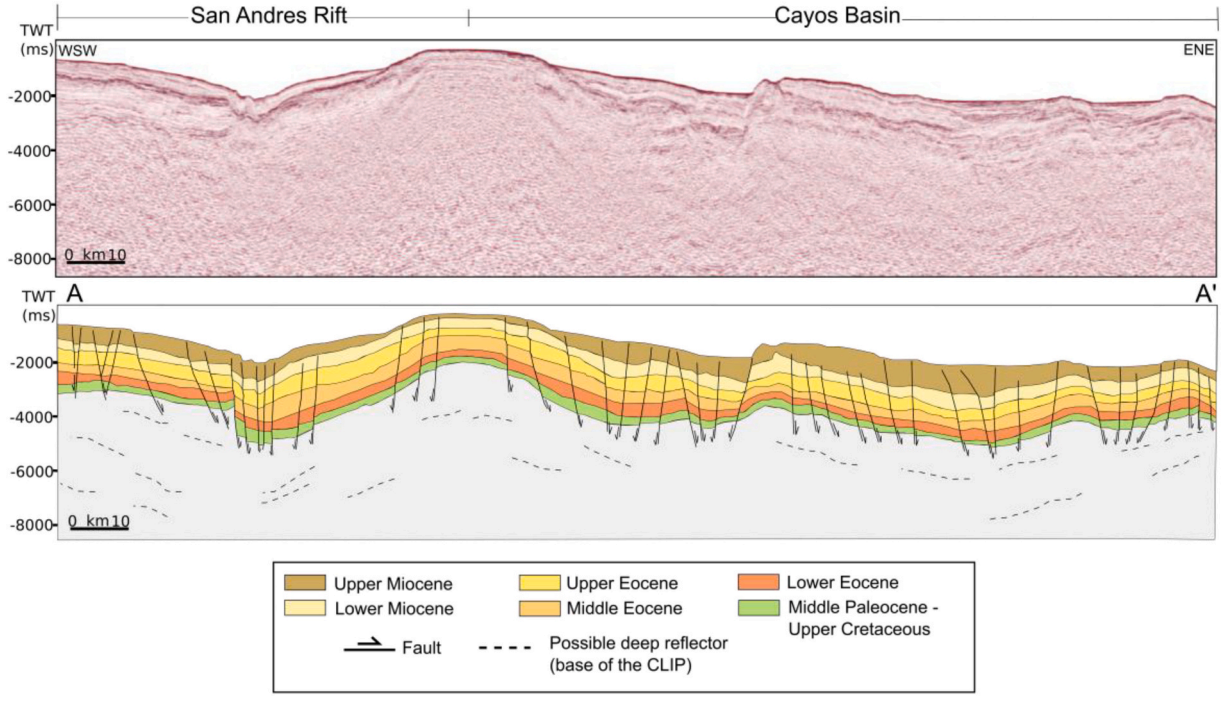

Fig. 3. Uninterpreted and interpreted seismic profile, west-southwest-trending, in two-way time (TWT), crossing the northwest part of the Cayos Basin. (From Carvajal Arenas and Mann, 2018). See Fig. 2 for location.

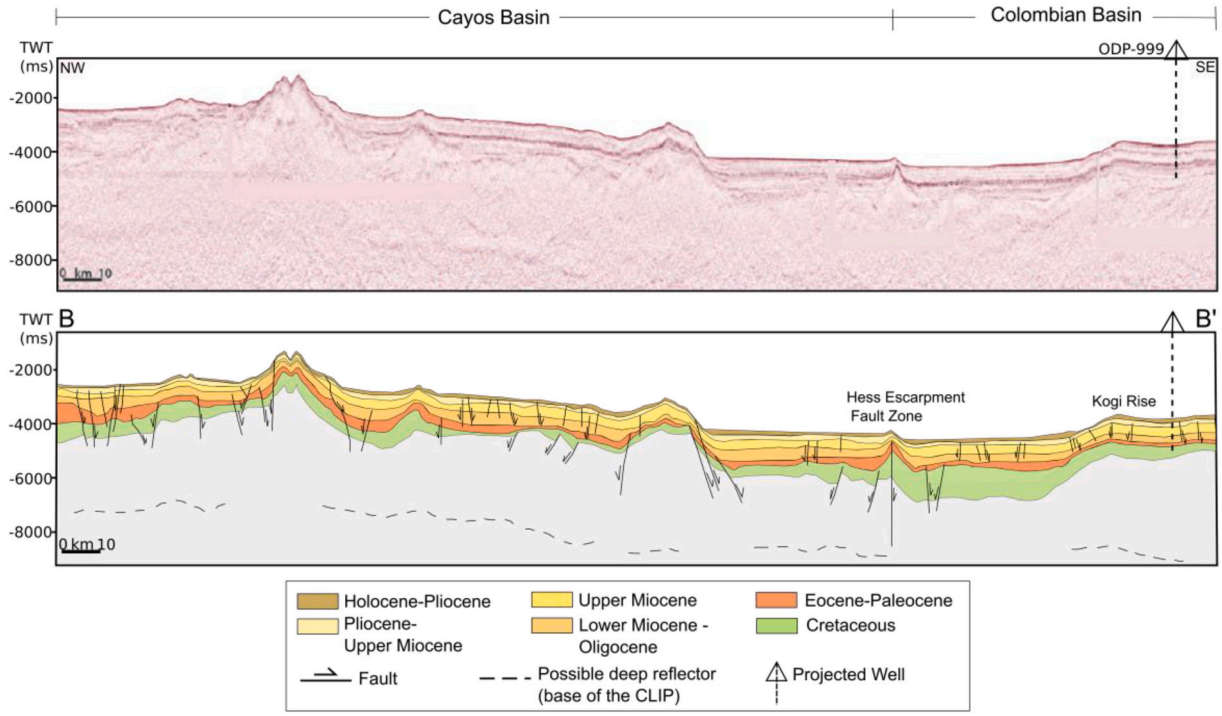

Fig. 4. NW-SE uninterpreted and interpreted seismic profile along the southern Cayos Basin, and the southeastern part of this profile crosses the western Colombian Basin. Depth in milliseconds, TWT (Two-Way travel Time). The seismic line is tied to the ODP-999 well in the Colombian Basin. (From Sanchez et al., 2019). See Fig. 2 for location.

bodies with standard values of density and magnetic susceptibility (Telford et al., 1976; Lowrie, 2007).

The development of the initial and reference model was based on known previous seismic (Ludwig et al., 1975; Carvajal Arenas, 2017; Sanchez et al., 2019) and drilling data (Abrams and Hu, 2000), as well as quantitative and qualitative gravity/magnetic data examination. Several values have been tested in order to provide reference starting values of the units, geometric and lithological constraints. The values were assigned to generate a signal that matched the observed data of the main lithology of the basin. Thus, the geometry of the polygons defined three main layers: sedimentary cover, crust, and mantle.

The profiles used for the crustal models were extracted from Free Air and the Reduce to the Pole anomalies. We proposed four scenarios for the Cayos Basin considering both affinities from the crustal in the basin (oceanic and continental). The main parameters used included: 1) average crustal and sediment thicknesses: Previous refraction studies suggest that the Upper Nicaraguan Rise has a crustal thickness of 20–25 km (Edgar et al., 1971). The Lower Nicaraguan Rise is underlain by a basement, with a thickness of approximately 15–20 km (Mauffret and Leroy, 1997) and the Colombian Basin has an approximate crustal thickness of between 10 and 18 km (Ewing et al., 1960; Ludwig et al., 1975). Additionally, Carvajal Arenas (2017) presented the Isostatic Moho Depth (IMD), a gravity inversion based on the isostatic equilibrium and the Archimedes principle, the IMD has an excellent fit with refraction methods, for determining the crustal thickness of the western Caribbean Sea. Together with the Nicaraguan Rise, Carvajal Arenas (2017) estimated the local marine stratigraphic sections to be over 8 km thick, characterized by local basins bound by volcanic basement highs.

2) Sediment, crustal, and mantle densities: For the density model, three density values of the crust were taken into consideration, oceanic crust (2900 kg/m^3), upper continental crust (2700 kg/m^3), and lower continental crust (2850 kg/m^3). Two sedimentary layers, with densities of 2200 and 2400 kg/m^3, provided the sedimentary infill, with 1027 kg/m^3 seawater and 3300 kg/m^3 for the mantle.

3) Parameters of the magnetic field: we included three magnetized layers: oceanic crust (0.008 SI units), upper continental crust (0.0035 SI units), and lower continental crust (0.004 SI units). We conventionally consider that all anomalies are the results of the Earth's permanent magnetic field induction into the rocks containing magnetic minerals. Therefore, the magnetic anomalies were modeled with a magnetic field intensity of 36,251 nT, an inclination of 41.4°, and a −4.7169° declination.

Finally, our modeling is based solely on induced magnetization. According to Shive (1989), the probability is high that a body that has been exposed to lower crustal conditions for 80 million years, will acquire a viscous magnetization. The viscous magnetization of a body in the lower crust will be acquired in such a way as to push the total magnetization towards a value of about 0.26fH, where f is the volume fraction of magnetic material, and H is the external field (Carmichael, 2017). For any rock containing magnetite as the dominant magnetic material, that value is about 25% greater than the induced magnetization of the rocks above located in the upper crust (Schlinger, 1985; Williams et al., 1985; Shive and Fountain, 1988; Shive et al., 1988). Thus, the remanent magnetization of the lower crustal rocks is not likely to contribute, significantly, to long-wavelength magnetic anomalies (Shive, 1989).

On the other hand, paleomagnetic studies to estimate the paleolatitude of the Caribbean region, over the past 80 million years, obtained during Leg 165 from Site 1000 (See Fig. 2 for location), include remanence measurements of split-core sections (typically 1.5 m long). Results displayed weak natural remanent magnetizations, typically $<8 \times =10^{-4}$ A/m (Acton et al., 2000). We use these paleomagnetic values in our forward modeling, although data from this site do not provide any constraints and are not considered. An anomalous total magnetization of lower-crustal blocks cannot be explained by suitable values of the induced magnetization alone, which also implies an influence of remanent magnetization (Maystrenko et al., 2017). However, due to the very deep location of the lower-crustal rocks, no data for remanent declination and inclination are available.

According to Maystrenko et al. (2017), there is also uncertainty

associated with the magnetic properties of the deep blocks, which are directly related to the Curie temperature, or Curie Point, where crustal rocks lose their magnetic properties. The case of the Cayos Basin in the Western Caribbean Plate, Quintero et al. (2019) shows that the Curie isotherm lies between 13 km and 27 km, assuming that the isotherm is located in the lower crust.

4. Results: Crustal configuration of the Cayos Basin from the potential field analysis

4.1. Analysis of magnetic and gravity anomalies

4.1.1. Gravity data analysis

Variations in gravity anomalies are shown on the Free-Air, Bouguer, and Residual Bouguer grids (Fig. 5).

These datasets were gridded at a grid increment of 1 km. By definition, the Free-Air anomalies register the combined vertical terrain gravity effect and the rooted gravity effect. In this case, the free-air gravity anomalies are partially produced by the density contrast between the seawater and the bedrock of the seafloor. Hence, some of these anomalies are directly correlated with the bathymetry, suggesting that the root effect can be discounted. The Free-Air grid (Fig. 5A) reveals that the Cayos Basin is dominated by a mixture of positive gravity (~141 mGal) anomalies and negative gravity (−63 mGal) anomalies. As can be seen, well-defined edges of circular geometries and positive wavelengths characterize the basin, showing correlation with numerous islands and coral banks (e.g., Cayos de Roncador, San Andrés, Cayos de Este Sudeste and Cayos de Albuquerque). Circular geometries with negative wavelengths reveal the main depressions. It is evident in the San Andres Rift, where negative anomalies (−60 mGal) show correlation con this feature mapped in the bathymetry (Fig. 5A). Towards the Colombian basin, the correlation with bathymetry is not obvious. The anomalies reveal positive values that reach ~141 mGal under the Colombian basin. Considering that we used a reduction density of 2670 kg/m^3 for the Bouguer correction, the positive values of the Bouguer anomaly observed (Fig. 5B) (pink/magenta tones), indicate the presence of bodies denser than the reference value. Negative values would correspond to lighter rocks. In general, the Bouguer gravity anomaly map reflects that the gravitational field increases in the southeast direction.

A third-order polynomial trend surface was removed from the Bouguer anomaly. As a result of the application of this technique, the residual anomalies elucidate the crustal density changes. The Residual Bouguer exhibits a value range of between −210 mGal and about 70 mGal. The gravity low values (−200 mGal) are found to the north-west in the vicinity of the Pedro Bank Fault Zone (dark blue tones) (Fig. 5C). In the Lower Nicaraguan Rise, anomalies present values between −13 mGal and 28 mGal (light green and yellow tones) (Fig. 5C). To the east, the results indicate maximum value anomalies in areas of the Colombian Basin, reaching gravity values up to 289 mGal (Fig. 5C). The residual gravity anomaly map suggests that the Cayos Basin is not a simple depression, but contains at least four separate sub basins (four different gravity minima). The regions with short wavelengths and negative Residual Bouguer (blue colors) are indicative of these smaller depocenters (Fig. 5C). A discontinuous lineament with high values (~20 mGal) is present towards the eastern area of the San Andres Rift.

4.1.2. Magnetic data analysis

In this section, we present the regional interpretation of magnetic data. The total field magnetic map (Fig. 6A) shows values ranging between −726 nT and 545 nT, with an average of −49 nT. In order to minimize the polarity effects, we applied the Reduction to the Pole to the total magnetic field. Anomalies interpreted from the total magnetic field are now become larger anomalies after the filter was applied, showing a range from −944 to 697 nT (Fig. 6B). The reduce to the pole shows that most of the Cayos Basin is characterized by short wavelengths and high amplitudes as large as 300 nT (pink/magenta tones). Negative amplitudes are found between these magnetic highs and correspond to small sub-basins. The Upper Nicaraguan Rise can be identified by the contact of positive long wavelengths (250 nT) against negative wavelengths (−350 nT). The magnetic signature in the Colombian Basin records striking *E*-W structures with positive (280 nT), and negative values (−470 nT).

The linear artifacts of small-scale magnetic anomalies crossing tectonic elements are primarily related to merging surveys. These elements are caused by data acquisition (shipboard tracks) at widely different times and by differences in merging procedures.

4.2. 2D forward modeling across the Cayos Basin in the LNR

The 2D forward modeling was carried out using GM-SYS software on both Free Air and the Reduce to the Pole anomalies, along three profiles (Fig. 2). The anomalies were calculated for polygon bodies, with standard values of density and magnetic susceptibility. Each value was assigned to generate a signal that matched the observed data of the main lithology of the Cayos Basin, and the geometry of the polygons defined three main layers: sedimentary cover, crust, and mantle. The structural styles in the profiles were carried out, based on seismic lines observations from previous works (Carvajal Arenas and Mann, 2018; Sanchez et al., 2019). In general, the seismic sections show a system of extensional faults involving the upper crust and sedimentary sections, where carbonate complexes are at the top of shallower basement highs. The 2D crustal models (Figs. 7, 8, 9, and 10) shed light on the deep crustal architecture of the region, and these were selected, based on their geographical location (Fig. 2), to a depth of 25 km.

Profile 1, oriented NW-SE (Fig. 7), was modeled with a length of 280 km and compared with the seismic profile (B–B′) (Fig. 4). The profile extends from the Cayos de Serrana Island to the northwest edges of the Kogi Rise with gravity ranging from 2 to 37 mGal. The magnetic values between −363 and 251 nT. The regional field shows significant variations at the Cayos de Serrana Island, in the center of the profile, and SE boundaries at the Kogi Rise, interpreted as basement highs in the LNR based on the seismic profile along Line B–B′(Fig. 4). Along the Cayos de Serrana Island, the profile shows an uplifted block with positive gravity (20 mGal) and magnetic (250 nT) anomalies. Towards the center, an uplifted block shows high gravity values (~35 mGal) and negative magnetic values (−360 nT). The Hess Escarpment Fault Zone displays free-air values that reaches 21 mGal (Fig. 7B) and the magnetic profile reaches ~75 nT. Towards the SE, areas with positive anomalies (28 mGal and 112 nT) are present at the northwest edges of the Kogi Rise. The Moho depth reaches approximately 17.5 km.

Profile 2, oriented NW-SE, was modeled with a length of 200 km (Fig. 8). The profile extends from the San Andres Rift to the Hess Escarpment Fault Zone and across Providencia Island. The gravity values show a range, from −24 mGals and 32 mGals, and magnetic values between −260 nT and 118 nT. The regional field shows gravity and magnetic variations at the NW and SE boundaries. Towards the NW over the San Andres Rift, profile show wavelength with negative amplitude (−24 mGals and −250 nT) where the seismic section A-A' (Fig. 3) shows a graben morphology with elevated Moho surface. Along the eastern rift shoulder of the San Andres Rift, the profile show positive gravity (26 mGals) and magnetic (20 nT) anomalies. Towards the SE, gravity and magnetic positive peaks represent the Hess Escarpment Fault Zone. The profile displays a signature of the free-air that reaches 32 mGals, and the magnetic field anomaly profile reaches approximately ~118 nT over the fault zone (Fig. 8). The Moho depth shows ranges from 17 to 18 km in the central part, and it's thinning in the San Andres Rift.

Profile 3, oriented SW-NE, is 300 km long (Fig. 9). The range of gravity values varies between −25 mGals and 37 mGals, and values of magnetic anomalies vary between −386 nT and 150 nT. The profile extends from the western edge of the Cayos Basin to the Cayos de Serrana Island and across Providencia Island. Gravity and magnetic

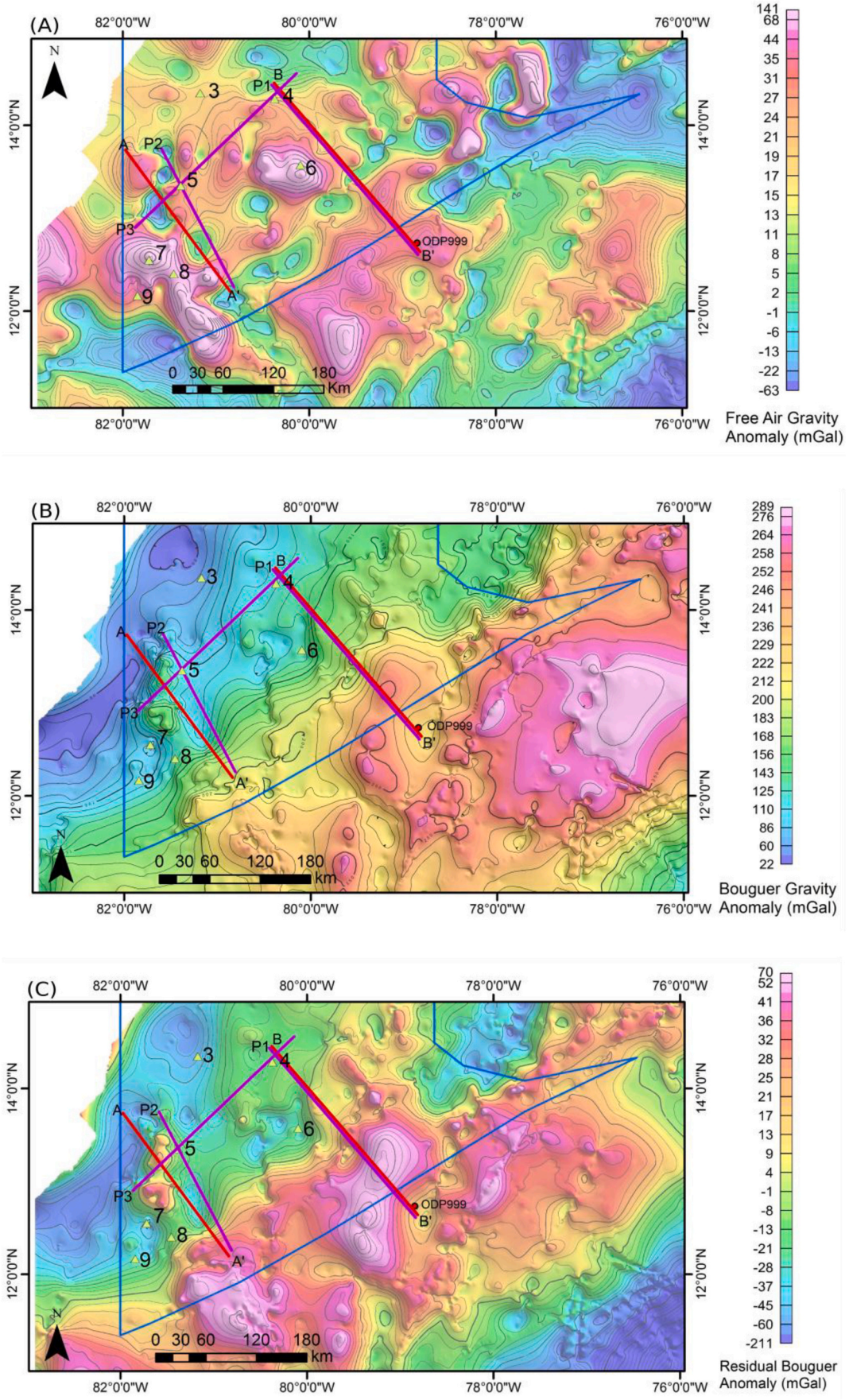

Fig. 5. Gravity grids of the Cayos Basin. (A) Free Air Anomalies. (B) Bouguer Anomalies. (C) Residual Bouguer Anomalies.

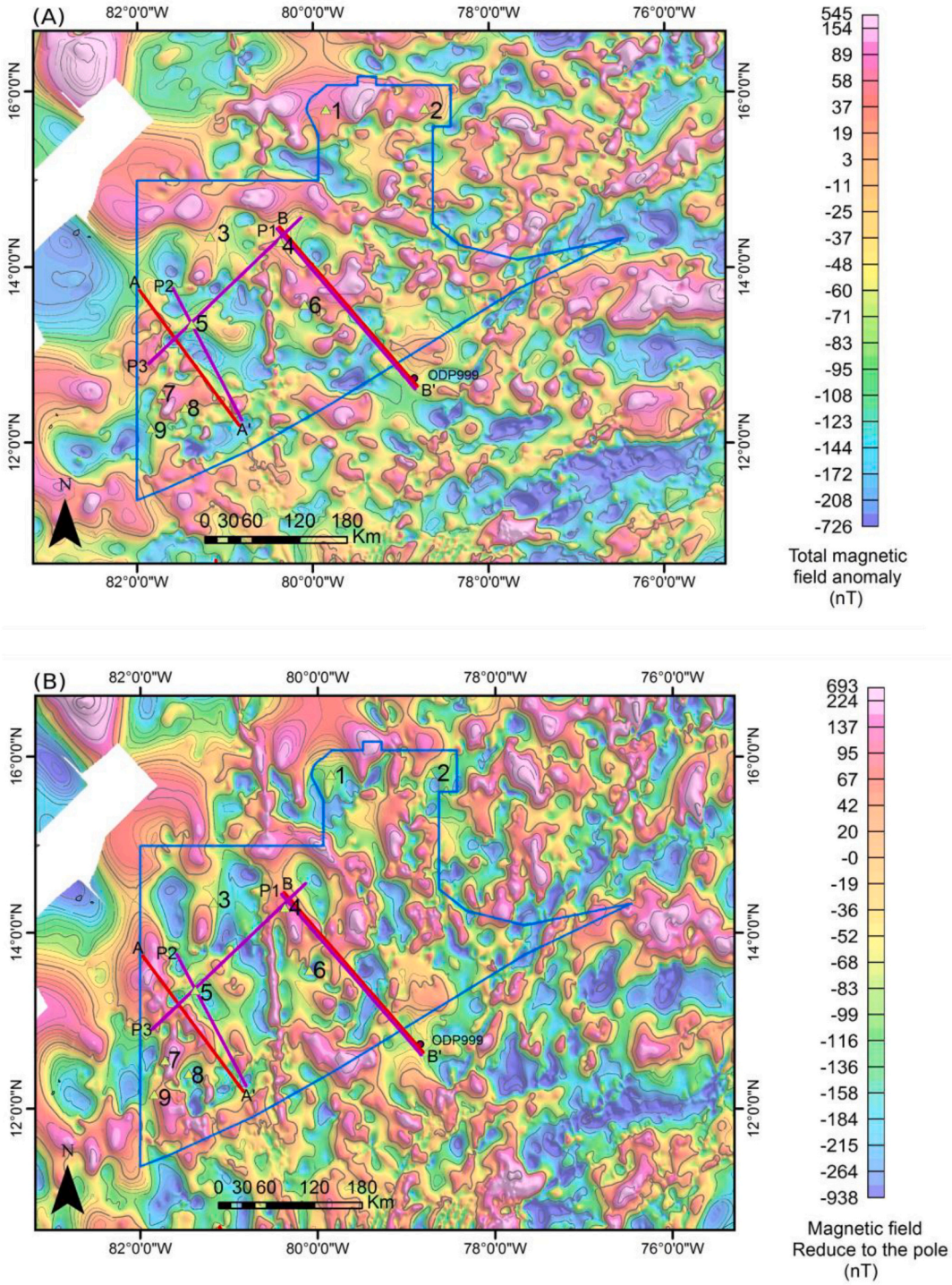

Fig. 6. Magnetic grids of the Cayos Basin. (A) Total Magnetic Field Anomalies (B) Reduce to the pole.

modeling along profile 2 (Fig. 9C) display a signature of the free-air gravity anomaly ranging from −25 to 38 mGal (Fig. 9B), and a magnetic field anomaly profile with values between −380 and 150 nT, with a significant magnetic anomaly low located in the center of the profile (Fig. 9A). Towards the SW, areas with negative anomalies (−25 mGals and −270 nT) are present in the San Andrés Rift. The San Andres Rift, in the eastern shoulder, shows a block that exposes Providencia Island, with anomalies that display high gravity values (~37 mGal) and positive magnetic values (~22 nT). Towards the eastern edge, a long-wavelength tendency shows the emerged area that conforms to Cayos de Serrana Island. This morphological structure corresponds to an uplifted block where the basement has well-defined edges and positive amplitudes in the anomalies. Another peak at the central part of the profile generates negative value magnetic anomalies. Here, smaller, local basins with important sedimentary infill are formed between uplifted blocks. The Moho depth reaches approximately 18 km, showing a thinning in the San Andres Rift, with a thickness of 15 km.

We attempted to reduce the level of misfit between observed and calculated data. In general, the misfit between observed and calculated gravity and magnetic values can occur for three reasons: 1) the assumed rock density and susceptibility values may be inaccurate; 2) the rock units may not be homogeneous in density and magnetization, and, 3)

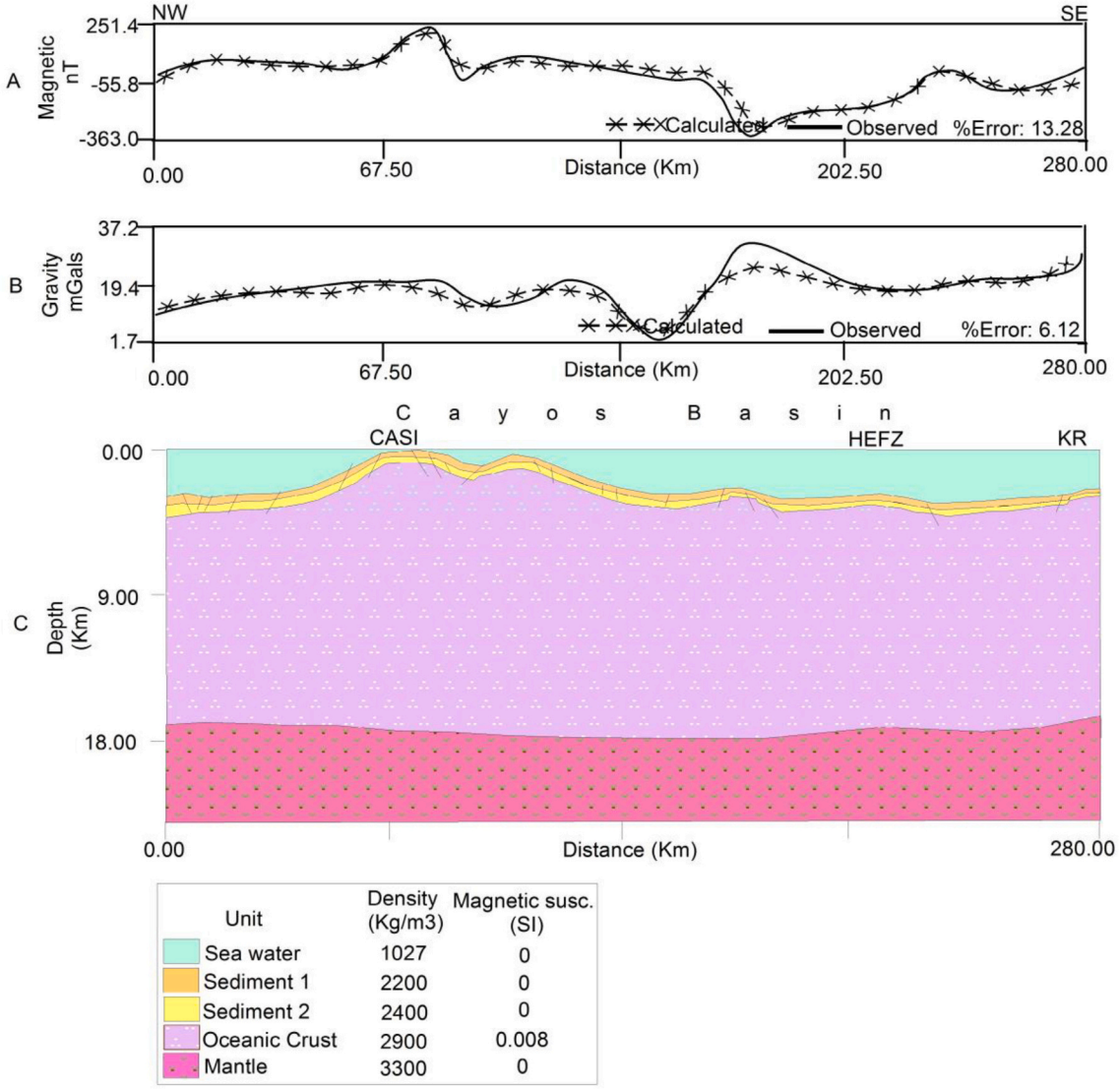

Fig. 7. Profile 1. A. Observed and calculated gravity anomalies. B. Observed and calculated magnetic anomalies. C. Gravity and magnetic forward model. Abbreviations: CASI: Cayos de Serrana Island. HEFZ: Hess Escarpment Fault Zone. KG: Kogi Rise. See Fig. 2 for location.

there may still be uncertainty in the boundaries of the rock units. In this work, we achieved an acceptable level of misfits, using average density and susceptibility values, and kept the geologic control of boundaries with the seismic profile.

5. Interpretation and discussion

Detailed analysis using the potential fields (gravimetric and magnetic anomalies) provides new knowledge of the crustal structure of the Cayos Basin in the LNR. Several authors still debate about the entire Nicaraguan Rise belonging to the Precambrian-Paleozoic continental Chortis block (Dengo, 1985; Krawinkel and Seyfried, 1994; Hradecky, 2011), or only the upper part to consist of thinned continental crust (Case et al., 1990; Mauffret and Leroy, 1997; Rogers et al., 2007). Some authors (e.g. Case et al., 1990; Holcombe et al., 1990a; Mauffret and Leroy, 1997; Muñoz et al., 1997) assume that the LNR may be composed of oceanic crust, but, in contrast, Mauffret and Leroy (1997) postulate that it belongs to the CLIP. The latest studies that include bathymetric mapping, sampling, and geochemical analyses, indicate that at least the northeast portion of the LNR and Hess Escarpment is of volcanic origin, and belong to the second stage formation of the CLIP (Dürkefälden et al., 2019).

In this study, gravity and magnetic measurements reveal numerous anomalous bodies with distinctive geophysical signatures below the Cayos Basin. An approach was applied using the Free Air Gravity Anomaly. The values revealed a mixture of positive (141 mGal), and negative (−63 mGal) gravity anomalies. The map shows correlation of various gravity highs with numerous islands, such as Cayos de Roncador, San Andrés, Cayos de Este Sudeste and Cayos de Albuquerque. Circular geometries, with well-defined edges, defined these high-density bodies. We related these patterns to submarine hills, assuming that their formation is associated with volcanic events on the seafloor, as indicated by Geister (1992) and MacMillan et al. (2004). Also, negative anomalies of the order of −60 mGal show correlation with the San Andres Rift features mapped in the bathymetry. Towards the Colombian basin, the correlation with bathymetry is not obvious. Here, the core of the Caribbean plate is largely composed of an over-thickened oceanic plateau with an atypical thickness (Edgar et al., 1971; Bowland, 1993; Kroehler et al., 2011). Therefore the Free-Air values reveal a mass excess under the basin as described by (Garzón-Moreno and Hernández-Pardo, 2018).

Our investigations indicate the presence of dense and highly magnetic geologic bodies. We analyze the subsurface density variations with Bouguer and Residual Bouguer anomalies. On the one hand, the Bouguer

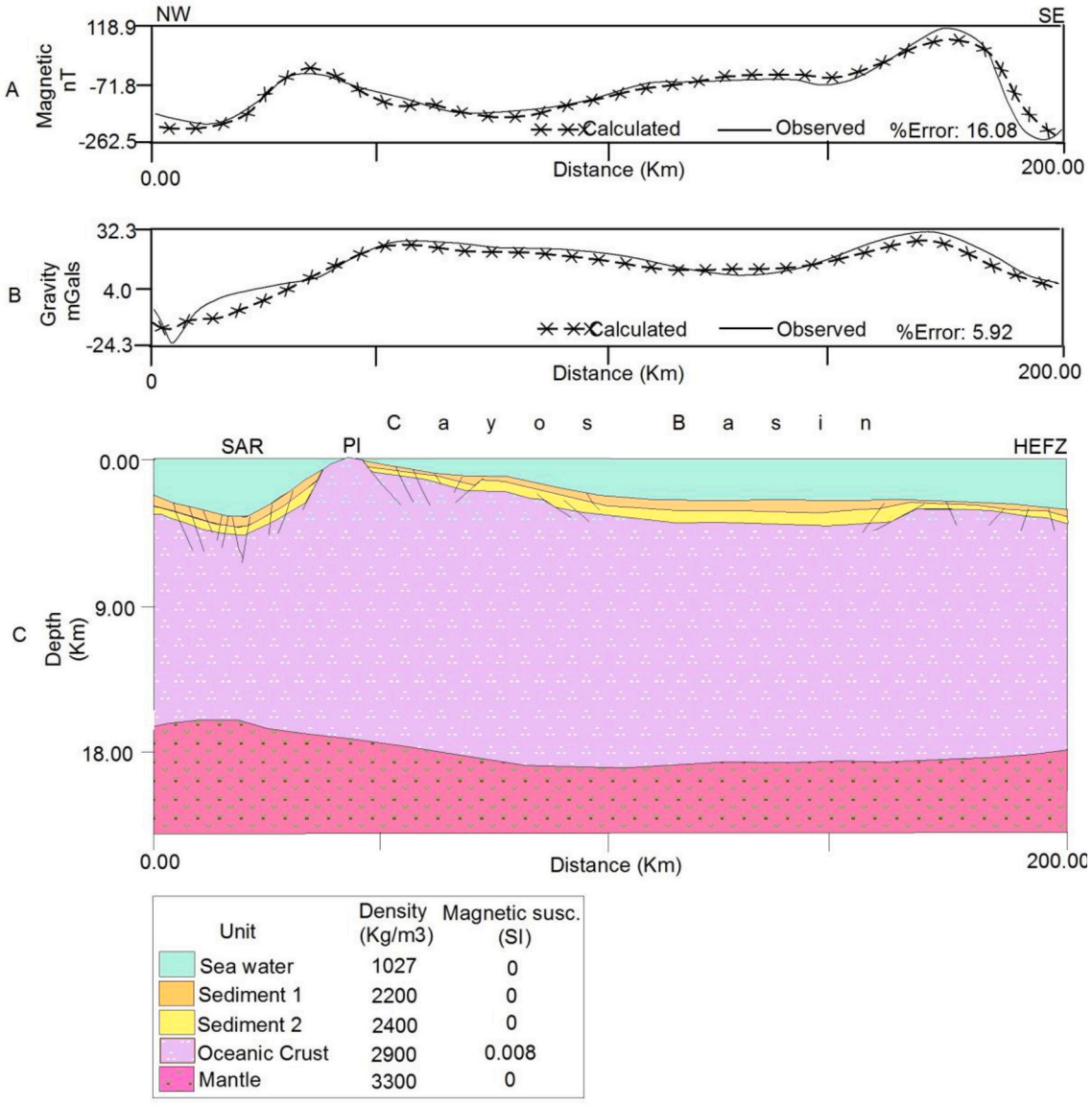

Fig. 8. Profile 2. A. Observed and calculated gravity anomalies. B. Observed and calculated magnetic anomalies. C. Gravity and magnetic forward model. The model displays a signature of the free-air gravity anomaly ranging from −24 mGals and 32 mGals, and a magnetic field anomaly profile with values between −262 nT and 118 nT. Abbreviations: HEFZ: Hess Escarpment Fault Zone. PI: Providencia Island. SAR: San Andres Rift. See Fig. 2 for location.

gravity anomaly show values ranging from 22 mGal y 289 mGal (Fig. 5B) and exhibit a decrease of the gravitational field in the northwest direction. The general decrease in the gravity field is due to the thinning of the crust (Buness et al., 1992; Jallouli and Mickus, 2000). In order to highlight the gravity anomalies caused by crustal density changes, the third-order polynomial surface was applied. The residual gravity anomalies obtained through the third-order polynomial surface, in general, reflect the configuration of the Moho surface (Buness et al., 1992). In the Cayos Basin, residual anomalies values between −13 mGal and 28 mGal, are evidence of higher density crustal and correlate better with the structural features. On the other hand, the magnetic signature of most of the Cayos Basin portrays a complex province, with circular shapes as large as 300 nT. The high magnetic anomaly amplitude, about 250 nT, supports a magnetization similar to a volcanic origin (de Moura et al., 2019), which could be related to the highly magnetic volcanic edifices found on the ocean floor. Milliman and Supko (1968) gathered geomagnetic data during a survey cruise to the San Andrés area, which indicated possible deep-seated volcanic bodies under the limestone caps of the atolls and San Andrés Island. Their volcanic origin was further supported by a basaltic pebble that was dredged from a depth of about 700 m at the Albuquerque Bank, during the same expedition. This corroborates the volcanic origin of the Cayos Basin basement hypothesis, where edifices play an important role in the distribution of magnetized ground. To the east, the results exhibit high values of approximately 70 mGal, and agree with the structure of a thick oceanic crust under the Colombian basin, composed mainly of the CLIP (Burke et al., 1978; Burke, 1988). The magnetic signature records striking *E*-W structures. The amplitudes and the wavelengths of the anomalies are typical for a basaltic crust (Werner et al., 2011), related to the development and growth of the CLIP, by the Late Cretaceous.

To determine the thickness and affinity of the crustal block below the Cayos Basin, four 2D gravity/magnetic forward models were performed, using Free Air and Reduce to the Pole profiles. Profiles 1, 2, and 3 considered Cayos Basin as a homogeneous oceanic crust, with crustal thickness changes from the thinned oceanic crust (15 km) in the San Andres Rift, to a thick oceanic crust (17–18 km). The error observed between gravity and magnetic modeling for Profile 1, NW-SE (Fig. 7), was 6.12% and 13.28%, respectively. Profile 2 (Fig. 8) shows a 16.08%

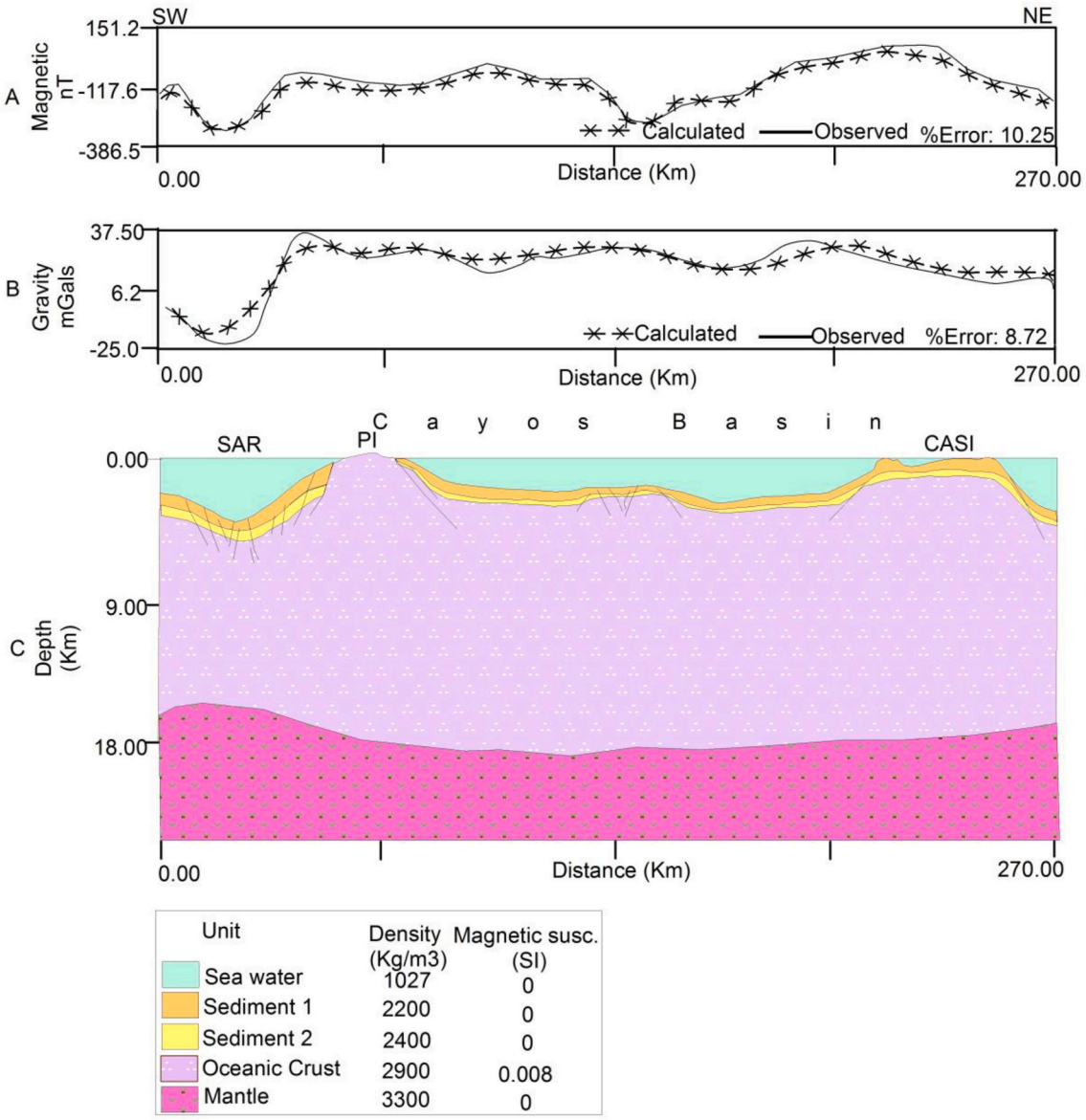

Fig. 9. Profile 3. A. Observed and calculated gravity anomalies. B. Observed and calculated magnetic anomalies. C. Gravity and magnetic forward model. The range of gravity values varies between −25 mGals and 37 mGals, and values of magnetic anomalies vary between −386 nT and 150 nT. Abbreviations: CASI: Cayos de Serrana Island. PI: Providencia Island. SAR: San Andres Rift. See Fig. 2 for location.

error observed in magnetic anomalies, and 2.92% in gravity anomalies. Finally, profile 3 (Fig. 9), displays an error of 10.25% and 8.72% for the magnetic and gravity response, respectively.

The differences between observed and modeled data reveal a complex structure, however, we assume that the long-wavelength anomalies present in the observed data are originated from a basement structure. Positive wavelengths probably characterize geological sources with density and high magnetization.

We evaluated an alternative approach for a crustal structure, where we assume that the Cayos Basin consists of thinned continental crust (Fig. 10). The model was tested along with profile 3, SW-NE (See Fig. 2 for location), with changing density and susceptibility values associated with a continental crustal type. The observed and modeled curves in this alternative model do not match, and present an error of 95.73% and 93.48%, in magnetic and gravity anomalies, respectively. We discarded this approximation and considered profiles 1, 2, and 3 as the most accurate. Where an oceanic crust is represented, gravity and magnetic signals are produced that better match the observed data.

6. Conclusions

An integrated geophysical analysis of potential fields (gravimetric and magnetic anomalies) of the Cayos Basin area in the Lower Nicaraguan Rise, indicates that there is a distinct variation in the crustal geometry. The presence of the basement surface suggests a depth of between 2 km and 6 km and the Moho discontinuity about 18 km below the Cayos Basin. An area of shallower Moho may indicate thinning of the crust below the San Andres Rift.

The variations in gravity and magnetic measurements indicate a heterogeneous structure and distinctive geophysical signatures below the Cayos Basin and surrounding areas. Gravity lows of as much as −200 mGal are found along the Pedro Bank Fault Zone, and intermediate high gravity anomalies are evidence of a higher density that extends throughout the Cayos Basin to the Colombian Basin. Magnetic anomalies clearly defined the heterogeneity in the magnetic susceptibility of scattered rocks in the Upper and Lower Nicaraguan Rise.

The oceanic nature of the crust underlying the Cayos Basin is demonstrated by 2D gravity/magnetic forward models, where modeled

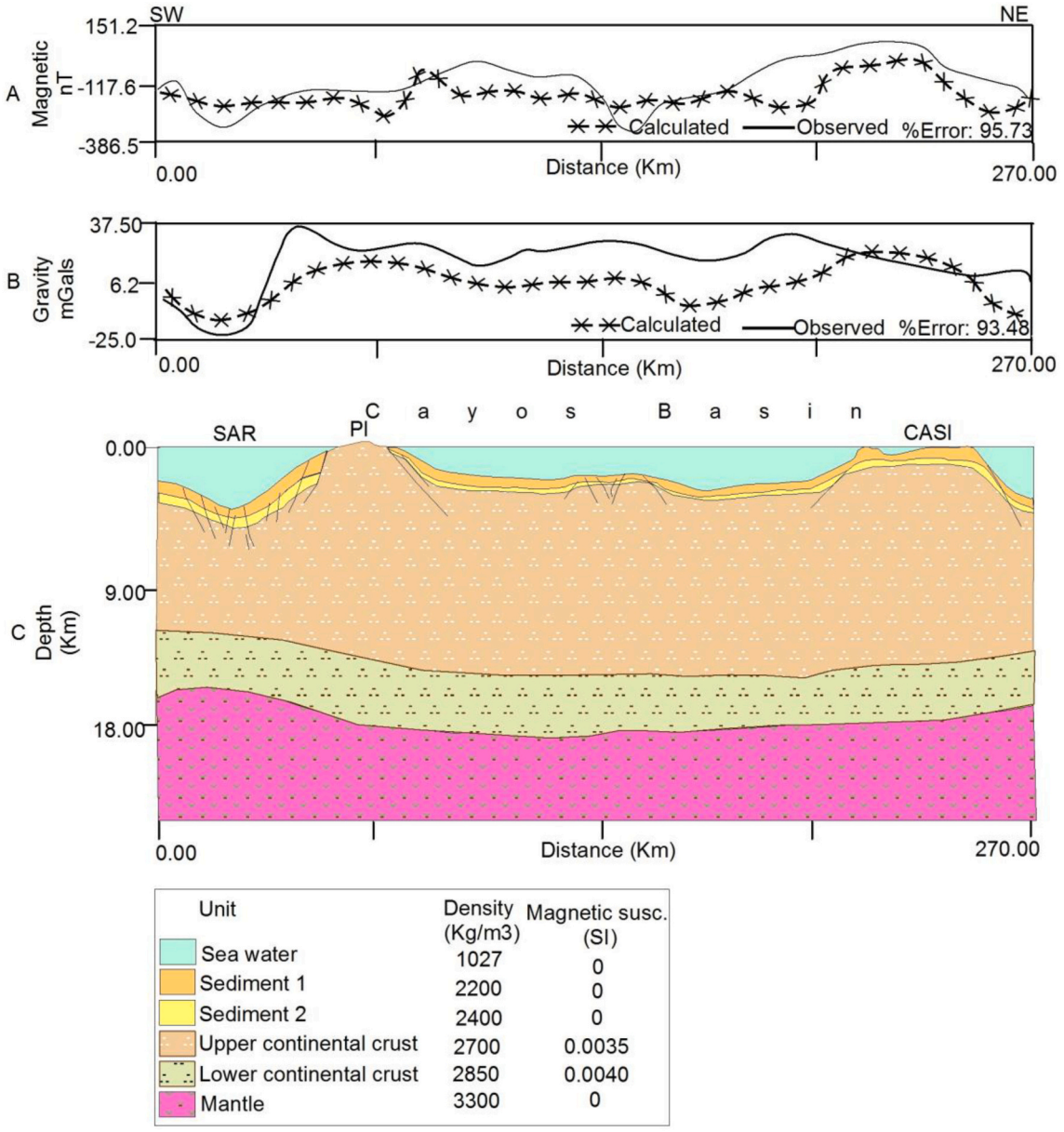

Fig. 10. 2D forward modeling of gravity and magnetic data showing an alternative approach for a crustal structure, where thinning of the continental crust underlying the Cayos Basin is observed. A. Observed and calculated gravity anomalies. B. Observed and calculated magnetic anomalies. C. Gravity and magnetic forward model. Observed and modeled curves in profile 3 do not match, and present an error of 95.42% and 93.64% in magnetic and gravity anomalies, respectively. See Fig. 2 for location.

data signals more closely matched the observed data than when considering a continental crust. We show that the region is of oceanic affinity, arguing against the assumption that the area may be part of the continental Chortis block, with it being more consistent that it pertains to the CLIP.

Our results are consistent with the seismic predictions of an oceanic crust below the Cayos Basin, rather than the continental Chortis block, confirming the suggestion of Mauffret and Leroy (1997) and Dürkefläden et al. (2019).

Data availability

Gravimetric, magnetic, and bathymetry data used in this study are publicly available in Zenodo Repository (DOI: https://doi.org/10.5281/zenodo.4035173) and at URL: https://zenodo.org/badge/DOI/10.5281/zenodo.4035173.svg.

Declaration of Competing Interest

The authors declare that they have no known competing financial interests or personal relationships that could have appeared to influence the work reported in this paper.

Acknowledgments

The authors thank the Colombian National Hydrocarbon Agency and the U. S. Geological Survey for providing geophysical datasets. We also thank the National University of Colombia for the academic licenses used for analyzing and modeling. The APC was funded by the University of Cadiz (UCA) through the UCA Own Research Plan and funds from the RNM912 Coastal Engineering Research Group. We also thank the Editor-in-Chief Michele Rebesco, Yuriy P. Maystrenko, and anonymous reviewers for their valuable comments which greatly improved the

manuscript. We also wish to acknowledge Edward Osorio of the Instituto de Investigaciones en Estratigrafía (IIES), from the Universidad de Caldas, for his comments and suggestions in the production of this paper. Finally, our thanks go to Dr. Wilson Quintero (Servicio Geológico Colombiano) for his helpful suggestions and discussions.

References

Abrams, L.J., Hu, M., 2000. 13. Data Report: Depth to Volcanic Basement at Site 999. Kogi Rise, Colombian Basin.

Acton, G.D., Galbrun, B., King, J.W., 2000. 9. Paleolatitude of the Caribbean Plate since the late cretaceous. Atlantic v. 25, 25.

Amante, C., Eakins, B.W., 2009. ETOPO1 Arc-Minute Global Relief Model: Procedures, Data Sources and Analysis.

Arden Jr., D.D., 1969. Geologic History of the Nicaraguan Rise.

Bankey, V., Cuevas, A., Daniels, D., Finn, C.A., Hernandez, I., Hill, P., Kucks, R., Miles, W., Pilkington, M., Roberts, C., 2002. Digital Data Grids for the Magnetic Anomaly Map of North America.

Barrero, D., Pardo, A., Vargas, C.A., Martínez, J.F., 2007. Colombian sedimentary basins: nomenclature, boundaries and petroleum geology, a new proposal. In: Agencia Nacional de Hidrocarburos, ANH and B&M Exploration Ltd Bogotá, 1, p. 92.

Berrocoso, M., Gárate, J., Martín-Dávila, J., Fernández-Ros, A., Moreu, G., Jigena, B., 1996. Improving the local geoid with GPS: Reports of the Finnish Geodetic Institute, v. 96, pp. 91–96.

Blakely, R.J., Simpson, R.W., 1986. Approximating edges of source bodies from magnetic or gravity anomalies. Geophysics 51, 1494–1498.

Boschman, L.M., van Hinsbergen, D.J.J., Torsvik, T.H., Spakman, W., Pindell, J.L., 2014. Kinematic reconstruction of the Caribbean region since the Early Jurassic. Earth Sci. Rev. 138, 102–136.

Bowland, C.L., 1993. Depositional history of the western Colombian Basin, Caribbean Sea, revealed by seismic stratigraphy. Geol. Soc. Am. Bull. 105, 1321–1345.

Bowland, C.L., Rosencrantz, E., 1988. Upper crustal structure of the western Colombian Basin. Caribbean Sea Geol. Soc. Am. Bull. 100, 534–546.

Buness, H., Giese, P., Bobier, C., Eva, C., Merlanti, F., Pedone, R., Jenatton, L., Nguyen, D.T., Thouvenot, F., Egloff, F., 1992. The EGT-85 Seismic Experiment in Tunisia-a reconnaissance of the deep structures. Tectonophysics v. 207, 245–267.

Burke, K., 1988. Tectonic evolution of the Caribbean. Annu. Rev. Earth Planet. Sci. v. 16, 201–230.

Burke, K., Fox, P., Şengör, A., 1978. Buoyant ocean floor and the evolution of the Caribbean. J. Geophys. Res. Solid Earth (1978–2012) 83, 3949–3954.

Carmichael, R.S., 2017. Magnetic properties of minerals and rocks. In: Handbook of Physical Properties of Rocks. CRC Press, pp. 229–288.

Carvajal Arenas, L.C., 2017. Hydrocarbon Prospectivity of the Nicaraguan Rise and Colombia Basin, western Caribbean Sea. University of Houston.

Carvajal Arenas, L.C., Mann, P., 2018. Western Caribbean intraplate deformation: defining a continuous and active microplate boundary along the San Andres rift and Hess Escarpment fault zone, Colombian Caribbean Sea. AAPG Bull. 102, 1523–1563.

Carvajal Arenas, L.C., Mann, P., Saunders, M., 2013. Petroleum prospectivity of the southwestern Nicaraguan Rise (Colombian Caribbean) based on regional integration of seismic and well data (abs.). In: AAPG Annual Convention and Exhibition, Pittsburgh, Pennsylvania, May 19–22, 2013.

Carvajal, L.C., Mann, P., 2015. Petroleum system analysis of the nicaraguan rise and colombia basin: a regional overview from seismic and well data. Search Discov. 10736.

Case, J.E., MacDonald, W.D., Fox, P.J., 1990. Caribbean crustal provinces; seismic and gravity evidence: the Caribbean Region, pp. 15–36.

Christofferson, E., Hamil, M.M., 1978. A radial pattern of sea-floor deformation in the southwestern Caribbean Sea. Geology v. 6, 341–344.

Cordell, L., 1992. A scattered equivalent-source method for interpolation and gridding of potential-field data in three dimensions. Geophysics 57, 629–636.

D'Acremont, E., Leroy, S., Burov, E.B., 2003. Numerical modelling of a mantle plume: the plume head–lithosphere interaction in the formation of an oceanic large igneous province. Earth Planet. Sci. Lett. 206, 379–396.

de Moura, D.S., Molina, E.C., Marangoni, Y.R., Jovane, L., 2019. Gravity and magnetic constraints on the crustal structure of the Ceará Plateau. Braz. Equator. Margin Front. Earth Sci. 7, 309.

Dengo, G., 1985. Mid America. Tectonic setting for the Pacific margin from southern México to northwestern Colombia. In: The Ocean Basins and Margins. Springer, pp. 123–180.

Dürkefälden, A., Hoernle, K., Hauff, F., Werner, R., Garbe-Schönberg, D., 2019. Second-stage Caribbean large igneous Province VOLCANISM: the depleted icing on the enriched cake. Chem. Geol. v. 509, 45–63.

Edgar, N.T., Ewing, J.I., Hennion, J., 1971. Seismic refraction and reflection in Caribbean Sea. AAPG Bull. 55, 833–870.

Ewing, J., Antoine, J., Ewing, M., 1960. Geophysical measurements in the western Caribbean Sea and in the Gulf of Mexico. J. Geophys. Res. 65, 4087–4126.

Garzón-Moreno, L.A., Hernández-Pardo, O., 2018. Estado isostático del abanico del rio Magdalena a partir de la interpretación de anomalías de campos potenciales, Cuenca Colombia. Bol. Geol. 40, 55–67.

Geister, J., 1992. Modern Reef Development and Cenozoic Evolution of an Oceanic Island/Reef Complex: Isla de Providencia (Western Caribbean Sea, Colombia), 27. Facies, p. 1.

Geister, J., Díaz, J., 2002. Ambientes Arrecifales Y geología de Un archipiélago oceánico: San Andrés, Providencia Y Santa Catalina: Mar Caribe, Colombia (Guía de Campo). INVEMAR, Santa Marta.

Heiskanen, W.A., Moritz, H., 1967. Physical Geodesy (Book on Physical Geodesy Covering Potential Theory, Gravity Fields, Gravimetric and Astrogeodetic Methods, Statistical Analysis, etc).

Hofmann-Wellenhof, B., Moritz, H., 2005. Fundamentals of potential theory. Phys. Geodesy 3–41.

Holcombe, T.L., Ladd, J.W., Westbrook, G.K., Edgar, N.T., 1990a. Caribbean marine geology; active margins of the plate boundary: The Caribbean Region. In: The Geology of North America, Vol. H. Geol. Soc. Am, Boulder, CO, pp. 261–290.

Holcombe, T.L., Ladd, J.W., Westbrook, G.K., Edgar, N.T., 1990b. Caribbean marine geology; ridges and basins of the plate interior: The Caribbean Region. In: The Geology of North America, vol. H. Geological Society of America, pp. 231–260.

Hradecky, P., 2011. Introduction to the special volume. J. Geosci. 56, 1–7.

Idarraga Garcia, J., Leon Rincon, H., 2019. Unraveling the underwater morphological features of Roncador Bank, Archipelago of San Andres, Providencia and Santa Catalina (Colombian Caribbean). Front. Mar. Sci. 6, 77.

Jallouli, C., Mickus, K., 2000. Regional gravity analysis of the crustal structure of Tunisia. J. Afr. Earth Sci. 30, 63–78.

Jigena, B., Berrocoso, M., Torrecillas, C., Vidal, J., Barbero, I., Fernandez-Ros, A., 2016. Determination of an experimental geoid at Deception Island, South Shetland Islands, Antarctica. Antarct. Sci. 28, 277.

Krawinkel, J., Seyfried, H., 1994. A review of plate-tectonic processes involved in the formation of the southwestern edge of the Caribbean Plate. Profil v. 7, 47–61.

Kroehler, M.E., Mann, P., Escalona, A., Christeson, G.L., 2011. Late Cretaceous-Miocene diachronous onset of back thrusting along the South Caribbean deformed belt and its importance for understanding processes of arc collision and crustal growth. Tectonics 30.

León Rincón, H., Pedroza Nieto, W.T., Vega Barbosa, G., 2019. El Territorio Integral e Indivisible del Archipiélago de San Andrés, Providencia y Santa Catalina. En Dimar. (2019). In: Book: Atlas Geomorfológico del Departamento Archipiélago de San Andrés, Providencia y Santa Catalina. Editorial Dirección General Marítima (DIMAR), 1ra. Ed.2019, pp. 205–253. ISBN: 978-958-5412-52-1.

Lowrie, W., 2007. Fundamentals of Geophysics. Cambridge University Press.

Ludwig, W.J., Houtz, R.E., Ewing, J.I., 1975. Profiler-sonobuoy measurements in Colombia and Venezuela basins, Caribbean Sea. AAPG Bull. 59, 115–123.

MacMillan, I., Gans, P.B., Alvarado, G., 2004. Middle Miocene to present plate tectonic history of the southern central American Volcanic Arc. Tectonophysics v. 392, 325–348.

Mann, P., Burke, K., 1990. Transverse intra-arc rifting: Palaeogene Wagwater belt, Jamaica. Mar. Petrol. Geol. 7 (4), 410–412. https://doi.org/10.1016/0264-8172(90)90018-C.

Marsden, D., 1989. Layer cake depth conversion, Part I. The Leading Edge 8, 10–14.

Mauffret, A., Leroy, S., 1997. Seismic stratigraphy and structure of the Caribbean igneous province. Tectonophysics 283, 61–104.

Mauffret, A., Leroy, S., 1999. Neogene intraplate deformation of the Caribbean plate at the Beata Ridge. In: Sedimentary basins of the world, 4. Elsevier, pp. 627–669.

Maystrenko, Y.P., Olesen, O., Ebbing, J., Nasuti, A., 2017. Deep structure of the northern North Sea and southwestern Norway based on 3D density and magnetic modelling. Norweg. J. Geol./Norsk Geologisk Forening. 97 (3), 169–210.

Menke, W., 2012. Geophysical data analysis: discrete inverse theory. In: MATLAB Edition, v. 45. Academic Press.

Milliman, J.D., Supko, P.R., 1968. On the geology of san andres island, western caribbean. Geol. Mijn 47, 102–105.

Muñoz, A., Baca, D., Artiles, V., Duarte, M., Barboza, G., 1997. Nicaragua: petroleum geology of the Caribbean margin. Lead. Edge 16, 1799–1806.

Ott, B., Mann, P., Saunders, M., 2013. Role of the offshore Pedro Banks left-lateral strike-slip fault zone in the plate tectonic evolution of the northern Caribbean. In: AGU Fall Meeting Abstracts.

Oviedo Prada, K., Jigena Antelo, B., Otálora Murillo, N., Romero Cózar, J., Contreras-de-Villar, F., Muñoz-Pérez, J.J., 2021. A new method for the collection of marine geomagnetic information: survey application in the Colombian Caribbean. J. Mar. Sci. Eng. 9, 10.

Quintero, W., Campos-Enríquez, O., Hernández, O., 2019. Curie point depth, thermal gradient, and heat flow in the Colombian Caribbean (northwestern South America). Geothermal Energy v. 7, 1–20.

Restrepo-Alvarez, J.J., Alvarez-Gutierrez, Y., Amaya_lópez, C., Barbosa-Mejía, L.N., Builes-Carvajal, J.S., Montoya-Cañola, S.M., Pacheco-Sintura, P.A., Ramirez-Hoyos, L.F., Urrego-Osorio, S., Zapata-Montoya, A.M., Ordoñez-Carmona, O., Henao-Casas, J.D., 2014. Descripción e interpretación geológica de las islas de Providencia y Santa Catalina. Boletín de Ciencias de la Tierra 35, 67–81. https://doi.org/10.15446/rbct.n35.39257.

Rey, W., Ruiz-Salcines, P., Salles, P., Urbano, C., Escobar-Olaya, G.A., Osorio, A.F., Ramírez-Monsalve, J.P., Cabarcas-Mier, A., Jigena-Antelo, B., Appendini, C.M., 2021. Hurricane Flood Hazard Assessment for the Archipelago of San Andres, Providencia and Santa Catalina, Colombia. Frontiers in Marine Sciences, 15 November 2021. https://doi.org/10.3389/fmars.2021.766258.

Rogers, R.D., Mann, P., Emmet, P.A., 2007. Tectonic terranes of the Chortis block based on integration of regional aeromagnetic and geologic data. Geol. Soc. Am. Spec. Pap. 428, 65–88.

Sanchez, J., Mann, P., Carvajal Arenas, L.C., Bernal-Olaya, R., 2019. Regional transect across the western Caribbean Sea based on integration of geologic, seismic reflection, gravity, and magnetic data. AAPG Bull. 103, 303–343.

Schlinger, C.M., 1985. Magnetization of lower crust and interpretation of regional magnetic anomalies: example from Lofoten and Vesterålen, Norway. J. Geophys. Res. Solid Earth 90, 11484–11504.
Shive, P.N., 1989. Can remanent magnetization in the deep crust contribute to long wavelength magnetic anomalies? Geophys. Res. Lett. 16, 89–92.
Shive, P.N., Fountain, D.M., 1988. Magnetic mineralogy in an Archean crustal cross section: Implications for crustal magnetization. J. Geophys. Res. Solid Earth 93, 12177–12186.
Shive, P.N., Frost, B.R., Peretti, A., 1988. The magnetic properties of metaperidotitic rocks as a function of metamorphic grade: implications for crustal magnetic anomalies. J. Geophys. Res. Solid Earth 93, 12187–12195.
Talwani, M., Heirtzler, 1964. Computation of magnetic anomalies caused by two dimensional structures of arbitary shape. In: Computers in the mineral industries, 1, pp. 464–480.
Telford, W.M., Geldart, L.P., Sheriff, R.E., Keys, D.A., 1976. Applied Geophysics. Cambridge University Press, Portland, ME, p. 860.
Wadge, G., Wooden, J.L., 1982. Late Cenozoic alkaline volcanism in the northwestern Caribbean: tectonic setting and Sr isotopic characteristics. Earth Planet. Sci. Lett. 57, 35–46.
Werner, R., Hoernle, K., Hauff, F., 2011. CLIP–Origin of the Caribbean Large Igneous Province (CLIP) in Connection with the Geodynamic Evolution of the Central Caribbean. Meteor-Berichte, pp. 11–18.
Williams, M.C., Shive, P.N., Fountain, D.M., Frost, B.R., 1985. Magnetic properties of exposed deep crustal rocks from the Superior Province of Manitoba. Earth Planet. Sci. Lett. v. 76, 176–184.